

Heat Transfer and Storage of Sodium Nitrate with Alumina Nanoparticles - Numerical Analysis.

M.Auriemma*, A.Iazzetta

Istituto Motori (CNR) Napoli

*Corresponding Author : M.Auriemma

ABSTRACT

New nanomaterials based on sodium nitrate and different concentrations (0.5%, 1% and 1.5% wt.) of alumina nanoparticles have been analyzed successfully via CFD. A numerical study on differences of thermo-physical properties of Phase Change Material (PCM) due to dispersion of alumina nanoparticles on sodium nitrate was produced. Transient numerical simulations with enthalpy porosity approach implemented in the commercial CFD-Code ANSYS FLUENT were performed.

An increase of the conductivity of the nano-enhanced Phase Change Material was predicted to lower charging and discharging cycles.

The specific heat was simulated at 529K (solid state) and 599K (liquid state). The melting temperature, the heat of fusion onset and crystallization temperatures of nanomaterials were compared with those of the base salt.

At the maximum concentration (1.5%), decrements of c_p were obtained at 529K and at 599K. In the case of the heat of fusion, a notable decrease was also predicted at the maximum concentration.

Keywords - Modeling, Specific Heat, Solar Salt, Nanoparticles, Thermal Energy Storage.

Date Of Submission: 27-12-2018

Date Of Acceptance: 11-01-2019

I. INTRODUCTION

The use of PCMs for TES is attracting great interest in recent years mainly for two reasons: the high amount of energy that is possible to store per unit of mass, and the fact that charging and discharging cycles take place at nearly constant temperature [1]. These features are of great importance, for thermodynamic reasons, in Direct Steam Generation where the liquid water/vapour transition occurs at a constant temperature.

Many research efforts were focused to the development of PCM-based energy storage systems for DSG. T. Bauer et al. studied [2] the thermophysical properties of sodium nitrate as PCM. The low conductivity of SN, 0.57 W/m K [3] in the solid state, is a serious drawback in order to use this material as PCM, especially during discharge cycles where the heat transfer through the solid layer is only by conduction. To overcome this problem, D. Laing et al. [4][5] proposed the use of aluminium fins to improve the heat transfer, and Wu & Zhao [6] proposed metallic foams and expanded graphite to increase the thermal conductivity of SN.

These solutions require complicated TES devices to achieve an adequate heat transfer rate. Other attempts have been focused on the design of PCM by the addition of nanoparticles.

Taking into consideration our past numerical studies [7] [8] on variations of thermo-physical properties of PCM due to dispersion of nanoparticles, in present work, we reinforced already copious experimental investigations with numerical investigation to estimate thermal performance of sodium nitrate due doping alumina nanoparticles. In literature in fact, [9] [10] [11] there is not good agreement between the different authors about effect of the addition of nanoparticles to the base salt. The discrepancies between authors maybe are due to the quality of dispersion of NP within the sodium nitrate. Moreover, the sizes of the nanoparticles play an important role on the possible improvement of the heat transfer properties of the base salt.

II. COMPUTATIONAL METHODOLOGY AND THERMAL PHYSICAL PROPERTIES

Property	SN	ANPs
Density (kg/m³)	2320-7.15e-1·T(K) [13]	3980 [14]
Specific heat (kJ/kgK)	1.776 (599 K) 2.431 (529 K)	
Conductivity (W/mK)	0.514 (liquid) [15] 0.57 (solid) [4]	1.471 (669 K) 1.237 (529 K) 1.195 (469 K) 20.2 (500 K) 15.8 (600 K) 12.6 (700 K)
Viscosity (mPa·s, cp)	0.1041·exp(1.63e-/(8.314T)) [13]	
Latent heat (kJ/kg)		
Melting temperature (K)	180 [2] 581 [2]	

Table 1. Thermo-physical properties of SN from existing literature or experimentally measured.

In the first place, numerical study about variations of thermo-physical properties of SN-based PCMs doped with alumina nanoparticles performed. In particular, we focused on numerical investigation of the melting and solidification of SN-based dispersed with three different concentrations (0.5%, 1% and 1.5% wt.) of alumina nanoparticles that is heated or cooled from one side of square enclosure of dimensions of 1 cm × 1 cm. The integrated simulation system ANSYS Workbench 15.0 for the numerical study was used including mesh generation tool ICEM and FLUENT software. In FLUENT, the melting and solidification model with volume of fluid (VOF) that includes the physical model to disperse nanoparticles in the PCM and their interactions is applied. During melting and solidification processes, the enhancement of heat transfer is considered. For this aim, the thermophysical properties of both starting materials (SN

and ANPs) were required as inputs. The values (Table 1) were obtained from existing literature. The geometry contains first sodium nitrate (SN) end then sodium nitrate (SN) with different concentrations (0.5%, 1% and 1.5% wt.) of alumina nanoparticles (ANPs).

For charging process initial temperature of the nePCM is 571 K, two wall sides are at a constant temperature of 591, the other two walls are adiabatic. For discharging process, initial temperature of the nePCM is 591 K, two wall sides are at a constant temperature of 571, the other two walls are adiabatic.

III. PHYSICAL MODEL - GOVERNING EQUATION

Assumptions made:

- ✓ The flow is Newtonian, incompressible and laminar.
- ✓ The viscous dissipations are negligible.
- ✓ The physical properties of PCM are temperature-dependent.
- ✓ Heat transfer is both conduction and convection controlled.
- ✓ The volume variation resulting from the phase change is neglected.

2D model is used, neglecting 3D convection. With this hypothesis, the results may be considered almost real because the 3D convection duration is very short compared with the whole melting process.

PCM Storage System: Fluid flow, heat transfer and phase change of the PCM processes with nanoparticles are regarded in the storage system [7] [8] The governing conservation equations are:

Continuity equation:

$$\frac{\partial \rho}{\partial t} + \nabla \cdot (\rho \vec{U}) = 0 \quad (5)$$

Momentum equation:

$$\frac{\partial}{\partial t} (\rho \vec{U}) + \nabla \cdot (\rho \vec{U} \vec{U}) = -\nabla \cdot P + \rho \vec{g} + \nabla \cdot \vec{\tau} + \vec{F} \quad (6)$$

Where P is the static pressure, $\vec{\tau}$ is the stress tensor, and $\rho \vec{g}$ and \vec{F} are the gravitational body and external body forces, respectively.

Energy equation:

$$\frac{\partial (\rho H)}{\partial t} + \nabla \cdot (\rho \vec{U} H) = \nabla \cdot (K \nabla T) + S \quad (7)$$

where H is the enthalpy, T is the temperature, ρ is density, K is the thermal conductivity, \vec{U} is the velocity and S is volumetric heat source term and is equal to zero in the present study.

The total enthalpy H of the PCM was computed as the sum of the sensible enthalpy, h and the latent heat, ΔH. The latent heat content, in terms of the latent heat of the PCM, L is:

$$\Delta H = \beta L \quad (8)$$

Where β is liquid fraction and is defined as:

$$\beta = 0 \quad \text{if} \quad T < T_{solid}$$

$$\beta = 1 \quad \text{if} \quad T > T_{solid}$$

$$\beta = \frac{T - T_{solid}}{T_{liquid} - T_{solid}} \quad \text{if} \quad T_{solid} < T < T_{liquid} \quad (9)$$

The solution for temperature is essentially an iteration between the energy Eq. (7) and the liquid fraction Eq. (9). The enthalpy-porosity technique treats the mushy region (partially solidified region) as a porous medium. The porosity in each cell is set equal to the liquid fraction in that cell. In fully solidified region, the difference in the solidus and liquid temperatures defines the transition from solid to liquid phases during the melting of PCM. The density, specific heat capacity and latent heat of the nanoPCM were defined as follows [D]:

$$\rho_{npcm} = \phi \rho_{np} + (1 - \phi) \rho_{pcm} \quad (10)$$

$$c_{p_{npcm}} = \frac{\phi(\rho c_p)_{np} + (1 - \phi)(\rho c_p)_{pcm}}{\rho_{npcm}} \quad (11)$$

$$L_{npcm} = \frac{(1 - \phi)(\rho L)_{pcm}}{\rho_{npcm}} \quad (12)$$

Where φ is volumetric fraction of nanoparticle. The dynamic viscosity and thermal conductivity of the nePCM are given by the following:

$$\mu_{npcm} = 0.983 e^{(12.958\phi)} \quad (13)$$

Thermophysical Properties - The effective thermal conductivity of the nanoPCM, which includes the effects of particle size, particle volume fraction and temperature dependence as well as properties of the base PCM and the particle subject to Brownian motion, is given by:

$$K_{npcm} = \frac{K_{np} + 2K_{pcm} - 2(K_{pcm} - K_{np})\phi}{K_{np} + 2K_{pcm} + (K_{pcm} - K_{np})\phi} K_{pcm} + 5 \times 10^4 \beta_k \phi \rho_{pcm} C_{p_{pcm}} \sqrt{\frac{BT}{\rho_{np} d_{np}}} f(T, \phi) \quad (14)$$

Where B is Boltzmann constant, 1.381×10^{-23} J/K and

$$\beta_k = 8.4407 * (100\phi)^{-1.07304} \quad (15)$$

$$f(T, \phi) = (2.8217 \times 10^{-2} \phi + 3.917 \times 10^{-3}) \frac{T}{T_{ref}} + (-0.669 \times 10^{-2} \phi - 3.91123 \times 10^{-3}) \quad (16)$$

The first part of Eq. (14) was obtained directly from the Maxwell model while the second part accounts for Brownian motion, which causes the temperature

dependence of the effective thermal conductivity. Note that there is a correction factor in the Brownian motion term, since there should be no Brownian motion in the solid phase. Its value is defined as the same as for liquid fraction, β in Eq.(9). For the numerical study, the integrated simulation system ANSYS Workbench 15.0 is used. The platform includes mesh generation tool ICEM and FLUENT software. Order to reduce the computational time, first, a fine structured mesh near the boundary layer and an increasingly coarser mesh in the rest of the domain was generated, and then the mesh is exported into FLUENT for solving the governing equations. To investigate both about dispersed nanoparticles in the PCM that about their interactions, in FLUENT, the melting model together to volume of fluid (VOF) model are applied. For modelling the melting process, the enthalpy-porosity technique is used. In this technique, the melt interface was not tracked explicitly. The liquid fraction indicating the fraction of the cell volume that is in liquid form was computed at each iteration, based on an enthalpy balance. The mushy zone is the region where the porosity increases from 0 to 1 as the PCM melts. To account for temperature dependence, the input parameters of PCM and of nanoparticles were defined using different user-defined functions (UDF) written in C++ language. The PRESSURE BASED method with the FIRST ORDER UPWIND differencing scheme were used for solving the momentum and energy equations, whereas the PRESTO scheme is adopted for the pressure correction. The under-relaxation factors for the velocity components, pressure correction and thermal energy are 0.5, 0.3 and 1 respectively. Grid dependence test showed that the maximum difference of the PCM temperature at an identical time is within 0.01% between using 4000 cells and 4800 cells with a time step of 0.1 s. After mesh independence study, considering both accuracy and computing time, 4400 cells with a time step of 0.1 s are used in the computations.

IV. RESULTS AND DISCUSSION

Transient two-dimensional numerical simulations were implemented for sodium SN and SN doped with 0.5%, 1% and 1.5% by mass of alumina nanoparticles, during charging and discharging processes. The aim was to scan the influence of the addition of nanoparticles suspended in the PCM in relation to:

- The thermo-physical properties
- The heat transfer rate

Limitations and advantages of the addition of ANPs were analyzed.

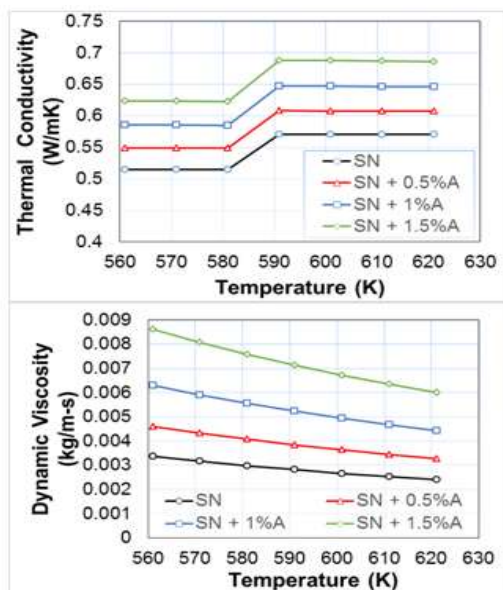


Fig. 1. Thermal conductivity (Top) and dynamic viscosity (Bottom) of SN-based PCMs doped with ANPs (0.5%,1% and 1.5% wt.)

Thermo-physical Properties As it can be seen in Figure 1, the thermal conductivity of SN-based PCMs doped with alumina nanoparticles is higher than the base salt SN. The higher the concentration of ANPs is the higher increment of thermal conductivity.

Hence, nePCMs have higher heat transfer rate compared to the same mass of non-doped PCM. Nonetheless, viscosity of SN-based PCMs doped with alumina nanoparticles increases with the mass concentration of ANPs, as shown in Figure 1(bottom). On one hand, the addition of ANPs to the base SN salt will lead to higher heat transfer rates and lower charging and discharging cycles. On the other hand, the higher dynamic viscosities for the ANPs-doped nanofluids will affect negatively to heat transmission by convection. These two effects will be considered in the simulation of a charging and discharging cycle.

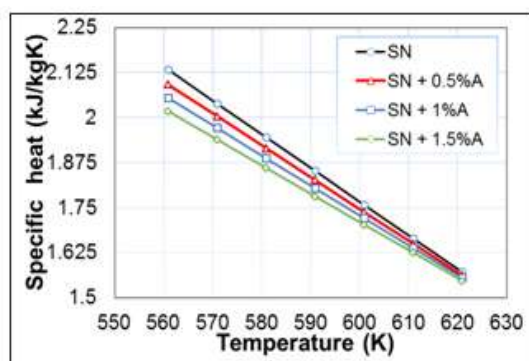


Fig. 2. Specific heat of SN-based nanofluids vs concentration of ANPs.

As it can be seen in Figure, the c_p of SN-based nanofluids with ANPs decreases with addition the concentration of ANPs. The differences are more notable at temperatures below the melting point. An important decrease of the latent heat that reached 13.9% for the higher concentration of ANPs (1.5% wt.) was predicted.

Heat transfer rate Figure 3 shows time evolution of charging (599 K) and discharging (529 K) of SN-based PCMs doped with ANPs at different concentrations (0.5%, 1% and 1.5% wt.). These temperatures were approximately 20K over the melting temperature and 50K below solidification temperature respectively.

Figure 3 displays that the charging and discharging cycles are slightly shortened with the addition of ANPs. This is mainly due to the enhancement of the thermal conductivity with the presence of ANPs (Figure 1 Top), despite of the lower convection heat transfers due to higher dynamic viscosities (Figure 2 bottom) for ANP-doped nanofluids. Discharging cycles are normally longer than charging ones because of the formation of a solid layer of lower conductivity that becomes a barrier to the heat conduction.

We ponder that these small improvements of the heat transfer performance simulated within a domain of 1cmx1cm can be considerably increased when higher volumes of PCM are used. In fact, soon, our investigations will continue, also considering varying PCM volume.

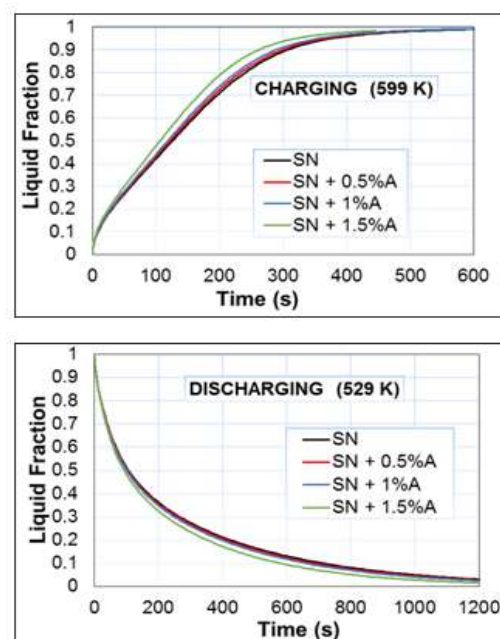


Fig. 3. Time evolution of charging (599 K) (Top) and discharging (529 K) (Bottom) of SN-based PCMs doped with ANPs at different concentrations (0.5%, 1% and 1.5% wt.).

Figure 3 shows the simulations for the cp at the two selected temperatures (529K and 599K) as well as the latent heat (kJ/kg). The cp of SN-based nanofluids decreases with the addition of ANPs in both the solid (529K) and liquid state (599K), however the decrease is more evident in the liquid state (599K). The latent heat also decreases with the addition of ANPs.

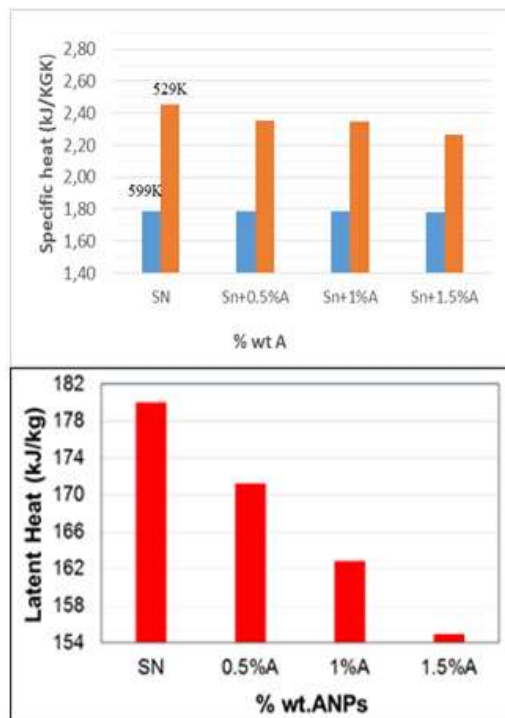


Fig.4. Top cp at two temperatures (529K and 599K), in the solid and liquid state for the SN and the three nanofluids of SN doped with ANPs (0.5, 1 and 1.5% wt.). Bottom Latent heat of SN-based nanofluids vs concentration of ANPs

The latent heat decreases constantly within the whole range of concentration of ANPs studied. An important decrease reached 13.9% for the higher concentration of ANPs (1.5% wt.) was predicted. It can be concluded that the addition of ANPs to SN does not improve the cp or the ΔH_f , but it makes the contrary effect. However, the simulations of the heat transfer rate showed an improvement in the performance of the nePCMs in the charging and discharging cycles due to an increase in the conductivity of the nanomaterial.

Based on the present study, we speculated that Sodium Nitrate with Alumina Nanoparticles enhanced the thermal conductivity. Still, thermal conduction mechanism in molten salt-based nanofluid needs to be further investigated.

V. CONCLUSION

A numerical study on differences of thermo-physical properties of Phase Change Material (PCM) due to dispersion of alumina nanoparticles on sodium nitrate was produced.

A complete cycle of charge and discharge was simulated using ANSYS Workbench 15.0, showing that the presence of ANPs increases the liquid fraction at specific times during charge, and decreases the liquid fraction during discharge. This fact could lead to shorten the charging and discharging cycles and to a better performance of the PCM during operation.

The presence of ANPs on SN-based PCMs does not improve the cp in the solid state (529K) and liquid state (599K) of the base salt. The results show no significant variation of this thermophysical property between 0 and 1% wt. of ANPs. However, a strong decrease is observed at 1.5% of ANPs. The ΔH_f decreases continuously with the concentration of ANPs in the whole range of concentration studied (0-1.5% wt.).

Advance theoretical modeling should be conducted to identify the specific tools affecting the specific heat of nanofluids as the concentration of nanoparticles changes. Current literature should be noticed to control if there is any uniformity in the results obtained when nanoparticles are added to fluids.

VI. ABBREVIATIONS

CSP	Concentrated Solar Power
DSG	Direct Steam Generation
MSBNF	Molten salt-Based NanoFluids
PCM	Phase Change Material
nePCM	Nano-enhanced Phase Change Material
NP	NanoParticles
ANPs	Alumina NanoParticles
SN	Sodium Nitrate
TES	Thermal Energy Storage

REFERENCES

- [1]. Liu M, Steven Tay NH, Bell S, Belusko M, Jacob R, Will G, et al. Review on concentrating solar power plants and new developments in high temperature thermal energy storage technologies. *Renew Sustain Energy Rev* 2016;53: 1411–32. doi:10.1016/j.rser.2015.09.026.
- [2]. Bauer T, Laing D, Kröner U, Tamme R. Sodium nitrate for high temperature latent heat storage. *11th Int Conf Therm Energy Storage* 2009:1–8.
- [3]. Sharifi N, Wang S, Bergman TL, Faghri A. Heat pipe-assisted melting of a phase change material. *Int J Heat Mass Transf* 2012;55: 3458–

- 69.doi:10.1016/j.ijheatmasstransfer.2012.03.023.
- [4]. Laing D, Eck M, Hempel M, Johnson M, Steinmann W-D, Meyer-Gruenfeld M, et al. High Temperature PCM Storage for DSG Solar Thermal Power Plants Tested in Various Operating Modes of Water/Steam Flow. Sol PACES Conf 2012
- [5]. Laing D, Bauer T, Lehmann D, Bahl C. Development of a Thermal Energy Storage System for Parabolic Trough Power Plants With Direct Steam Generation. *J Sol Energy Eng* 2010; 132:021011.doi: 10.1115/1.4001472.
- [6]. Wu ZG, Zhao CY. Experimental investigations of porous materials in high temperature thermal energy storage systems. *Sol Energy* 2011;85:1371–80.
- [7]. Auriemma M. Iazzetta A. Numerical Analysis of Melting of Paraffin Wax with Al₂O₃, ZnO and CuO Nanoparticles in Rectangular Enclosure *Indian Journal of Science and Technology*, Vol 9(3), DOI: 10.17485/ijst/2016/v9i4/72601, January 2016n
- [8]. Auriemma M Energy Storage: CFD Modeling of Phase Change Materials for Thermal Energy Storage. *Int. Journal of Engineering Research and Application* ISSN : 2248-9622, Vol. 6, Issue 6, (Part -5) June 2016, pp.31-36
- [9]. Betts M. The Effects of Nanoparticle Augmentation of Nitrate Thermal Storage Materials for Use in Concentrating Solar Power Applications. Texas A&M University, 2011.
- [10]. Chieruzzi M, Cerritelli GF, Miliozzi A, Kenny JM. Effect of nanoparticles on heat capacity of nanofluids based on molten salts as PCM for thermal energy storage. *Nanoscale Res Lett* 2013;8:448.
- [11]. Lasfargues M. Nitrate Based High Temperature Nano-heat-transfer-fluids: Formulation & Characterisation. University of Leeds (Institute of Particle Science & Engineering (IPSE) School of Process, Environmental and Materials Engineering (SPEME)); 2014.
- [12]. Ltd MI. Zetasizer Nano Series User Manual 2004.
- [13]. Janz GJ, Krebs U, Siegenthaler HF, Tomkins RPT. Molten Salts: Volume 3 Nitrates, Nitrites, and Mixtures: Electrical Conductance, Density, Viscosity, and Surface Tension Data. *J Phys Chem Ref Data* 1972; 1.
- [14]. Iv JHL, Lienhard JH. A heat transfer textbook. *J Heat Transfer* 1986; 108:198.
- [15]. Nagasaka Y, Nagashima A. The thermal conductivity of molten NaNO₃ and KNO₃. *Int J Thermophys* 1991; 12:769–81. doi:10.1007/BF00502404.
- [16]. Powell RW, Ho CY, Liley PE. Thermal conductivity of selected materials. U.S. Dept. of Commerce, National Bureau of Standards; for sale by the Superintendent of Documents, U.S. Govt. Print. Off.; 1966.

M.Auriemma" Heat Transfer and Storage of Sodium Nitrate with Alumina Nanoparticles - Numerical Analysis." *International Journal of Engineering Research and Applications (IJERA)*, vol. 9, no.1, 2019, pp 48-53